

A Unifying Framework for Spectrum-Preserving Graph Sparsification and Coarsening

Gecia Bravo Hermsdorff^{*,1} & Lee M. Gundersen^{*,2}

**Both authors contributed equally to this work*

¹Princeton Neuroscience Institute, Princeton University, Princeton, NJ, 08544, USA

²Department of Astrophysical Sciences, Princeton University, Princeton, NJ, 08540, USA

Abstract

How might one “reduce” a graph? That is, generate a smaller graph that preserves the global structure at the expense of discarding local details? There has been extensive work on both graph sparsification (removing edges) and graph coarsening (merging nodes, often by edge contraction); however, these operations are currently treated separately. Interestingly, for a planar graph, edge deletion corresponds to edge contraction in its planar dual (and more generally, for a graphical matroid and its dual). Moreover, with respect to the dynamics induced by the graph Laplacian (e.g., diffusion), deletion and contraction are physical manifestations of two reciprocal limits: edge weights of 0 and ∞ , respectively. In this work, we provide a unifying framework that captures both of these operations, allowing one to simultaneously coarsen and sparsify a graph, while preserving its large-scale structure. Using synthetic models and real-world datasets, we validate our algorithm and compare it with existing methods for graph coarsening and sparsification. While modern spectral schemes focus on the Laplacian (indeed, an important operator), our framework preserves its inverse, allowing one to quantitatively compare the effect of edge deletion with the (now finite) effect of edge contraction.

*Correspondences should be addressed to: geciah@princeton.edu or leeg@princeton.edu

1 Introduction

Many of the most interesting structures and phenomena of our world are naturally described as graphs (eg,¹ brains, social networks, the internet, etc). Indeed, graph data are becoming increasingly relevant to the field of machine learning [2, 3, 4]. These graphs are frequently massive, easily surpassing our working memory, and often the computer’s relevant cache [5]. It is therefore essential to obtain smaller approximate graphs to allow for more efficient computation and storage. Moreover, graph reduction aids in visualization and can provide structural insights.²

Graphs are defined by a set of nodes V and a set of edges $E \subseteq V \times V$ between them, and are often represented as an adjacency matrix³ $\underline{\underline{\mathbf{A}}}$ with size $|V| \times |V|$ and density $\propto |E|$. Reducing either of these quantities is advantageous; graph “coarsening” focuses on the former, aggregating nodes while respecting the overall structure, and graph “sparsification” on the latter, preferentially retaining the important edges.

A variety of algorithms have been proposed to attain these goals, and a frequently recurring theme is to consider the graph Laplacian $\underline{\underline{\mathbf{L}}} = \underline{\underline{\mathbf{D}}} - \underline{\underline{\mathbf{A}}}$, where $\underline{\underline{\mathbf{D}}}$ is the diagonal matrix of node degrees. Indeed, it appears in a wide range of applications (enough to motivate the coining of the term “Laplacian paradigm”[6]). For example: its spectral properties can be leveraged for community detection [7]; it can be used to efficiently solve min cut/max flow problems [8]; and for undirected, positively weighted graphs (the focus of our paper), it induces a natural quadratic form (which can be used, eg, to smoothly interpolate functions over the nodes [9]).

Work on spectral graph sparsification focuses on the preservation of the Laplacian quadratic form $\underline{\mathbf{x}}^T \underline{\underline{\mathbf{L}}} \underline{\mathbf{x}}$, a popular measure of spectral similarity suggested by Spielman and collaborators

¹The authors agree with the sentiment of the footnote on page xv in [1], viz, omitting superfluous full stops to obtain a more efficient (yet similarly lossless) compression of, eg: videlicet, exempli gratia, etc.

²For example, a common theme in biological systems is the presence of complicated pathways that produce a relatively simple result (eg, protein activation pathways). Semantic understanding comes from the reduction of these subsystems to their resulting behavior (eg, X activates a chain that eventually inhibits Y).

³A quick notation note: underlines denote bundling of multiple scalars into a single object, where the number of underlines denotes the rank of the tensor (ie, a single underline for vectors, double for matrices). Subscripts have nothing to do with Einstein summation notation; they are contextually-defined adornments.

[10]. A key result is that any graph may be sparsified by subsampling its edges, with optimal probability proportional to their effective resistance [11] (a measure of edge importance defined via the Laplacian pseudoinverse). Work on graph coarsening, however, has not reached a similar consensus. While it has been recently proposed to measure similarity between the original and coarsened graph using an analogous restricted quadratic form [12], the objective functions used for coarsening do not explicitly optimize this quantity. For example, Jin & Jaja [13] use the lowest k eigenvectors of the Laplacian (those corresponding to global structure) as feature vectors to perform k -means clustering of the nodes, while Purohit et al [14] aim to minimize the change to the largest eigenvalue of the adjacency matrix.

While recent work has combined coarsening and sparsification [15], they were performed by separate algorithmic primitives, essentially analyzing the composition of the above algorithms. In this work, we capture both of these operations using a *single* objective function that naturally promotes the preservation of large-scale structure. Our primary contributions include:

1. An identification of infinite edge weight with edge contraction, highlighting the finite limit of the Laplacian pseudoinverse $\underline{\underline{\mathbf{L}}}^\dagger$ (Section 2);
2. A graph reduction framework that unifies graph coarsening and sparsification by explicitly preserving $\mathbb{E}[\underline{\underline{\mathbf{L}}}^\dagger]$ (Sections 3 and 4);
3. A measure of edge importance of independent interest, which could be used to analyze connections in real-world networks (Section 3);
4. A more sensitive measure of spectral similarity of graphs (Section 5); and
5. A demonstration that our framework preferentially preserves the large-scale structure (Section 5).

2 Why the Laplacian pseudoinverse?

Many computations over graphs involve solving $\underline{\underline{\mathbf{L}}}\underline{\underline{\mathbf{x}}} = \underline{\underline{\mathbf{b}}}$ for $\underline{\underline{\mathbf{x}}}$ [6]. Thus, the (algebraically) relevant object is arguably the Laplacian *pseudoinverse* $\underline{\underline{\mathbf{L}}}^\dagger$, and in fact it has been used to derive useful measures of graph similarity [16]. Moreover, its largest eigenvalues are associated to global structure, thus, preserving the action of $\underline{\underline{\mathbf{L}}}^\dagger$ will preferentially maintain the overall shape of the graph. We now describe why $\underline{\underline{\mathbf{L}}}^\dagger$ is a natural operator to consider for both graph coarsening and sparsification.

Attention is often restricted to undirected, positively weighted graphs [17]. These graphs have many convenient properties, eg, their Laplacians are positive semi-definite ($\underline{\underline{\mathbf{x}}}^\top \underline{\underline{\mathbf{L}}} \underline{\underline{\mathbf{x}}} \geq 0$) and have a well-understood kernel and cokernel ($\underline{\underline{\mathbf{L}}}\underline{\underline{\mathbf{1}}} = \underline{\underline{\mathbf{1}}}^\top \underline{\underline{\mathbf{L}}} = \underline{\underline{\mathbf{0}}}$). The edge weights are defined as a mapping $W: E \rightarrow \mathbb{R}_{>0}$. When the weights represent connection strength, it is generally understood that $w_e \rightarrow 0$ is equivalent to removing edge e . However, the closure of the positive reals has a reciprocal limit, namely $w_e \rightarrow +\infty$.

This limit is rarely considered, as it can lead to divergences in many classical notions of graph similarity. A relevant example is the standard notion of spectral approximation, defined as preserving the Laplacian quadratic form $\underline{\underline{\mathbf{x}}}^\top \underline{\underline{\mathbf{L}}} \underline{\underline{\mathbf{x}}}$ to within a factor of $1 + \varepsilon$ for all vectors $\underline{\underline{\mathbf{x}}} \in \mathbb{R}^{|V|}$. Clearly, this limit yields a graph that does not approximate the original for any ε : any $\underline{\underline{\mathbf{x}}}$ with different values for the two nodes joined by edge e now yields an infinite quadratic form. This suggests considering only vectors that have the same value for these two nodes, essentially contracting them into a single “supernode”.

Algebraically, this interpretation is reflected in $\underline{\underline{\mathbf{L}}}^\dagger$, which remains finite in this limit: the pair of rows (and columns) corresponding to the contracted nodes becoming identical.

Physically, consider the behavior of the heat equation $\partial_t \underline{\underline{\mathbf{x}}} + \underline{\underline{\mathbf{L}}} \underline{\underline{\mathbf{x}}} = \underline{\underline{\mathbf{0}}}$: as $w_e \rightarrow +\infty$, the values on the two nodes immediately equilibrate between themselves, and remain tethered for the rest of the evolution.⁴

⁴In the spirit of another common analogy (edge weights as conductances of a network of resistors), breaking a resistor is equivalent to deleting that edge, while contraction amounts to completely soldering over it.

Geometrically, the reciprocal limits of $w_e \rightarrow 0$ and $w_e \rightarrow +\infty$ have dual interpretations: consider a planar graph and its planar dual; edge deletion in one graph corresponds to contraction in the other, and vice versa. This naturally extends to nonplanar graphs via their graphical matroid and its dual [18].

3 Our graph reduction framework

We provide a framework to construct probabilistic algorithms that generate a reduced graph \tilde{G} from an initial graph G , motivated by the following desirable properties:

1. reduce the number of edges and nodes,
2. preserve $\underline{\mathbf{L}}^\dagger$ in expectation,
3. minimize the change in $\underline{\mathbf{L}}^\dagger$.

In this section, we state these goals more formally, starting with a single iteration in its simplest form (ie, applied to a single, predetermined edge e).

3.1 Preserving the Laplacian pseudoinverse

Consider perturbing the weight of a single edge $e = (v_1, v_2)$ by Δw . The change in the Laplacian is simply

$$\underline{\mathbf{L}}_{\tilde{G}} - \underline{\mathbf{L}}_G = \Delta w \mathbf{b}_e \mathbf{b}_e^\top,$$

where $\underline{\mathbf{L}}_G$ and $\underline{\mathbf{L}}_{\tilde{G}}$ are the original and perturbed Laplacians, respectively, and \mathbf{b}_e is the signed incidence (column) vector associated to edge e , with entries

$$(b_e)_i = \begin{cases} +1 & i = v_1 \\ -1 & i = v_2 \\ 0 & \text{otherwise} \end{cases} \quad (1)$$

The change in $\mathbf{L}_{\equiv\equiv}^\dagger$ is given by the Woodbury matrix identity⁵ [20]:

$$\mathbf{L}_{\equiv\equiv\tilde{G}}^\dagger - \mathbf{L}_{\equiv\equiv G}^\dagger = -\frac{\Delta w}{1 + \Delta w \mathbf{b}_e^\top \mathbf{L}_{\equiv\equiv G}^\dagger \mathbf{b}_e} \mathbf{L}_{\equiv\equiv G}^\dagger \mathbf{b}_e \mathbf{b}_e^\top \mathbf{L}_{\equiv\equiv G}^\dagger,$$

Notice that this change can be expressed as a matrix that depends *only* on the choice of edge e , multiplied by a scalar term that depends (nonlinearly) on the perturbation to that edge:

$$\Delta \mathbf{L}_{\equiv\equiv}^\dagger = \underbrace{f\left(\frac{\Delta w}{w_e}, w_e \Omega_e\right)}_{\text{nonlinear scalar}} \times \underbrace{\mathbf{M}_e}_{\text{constant matrix}}$$

where

$$f = -\frac{\frac{\Delta w}{w_e}}{1 + \frac{\Delta w}{w_e} w_e \Omega_e}, \quad (2)$$

$$\mathbf{M}_e = w_e \mathbf{L}_{\equiv\equiv G}^\dagger \mathbf{b}_e \mathbf{b}_e^\top \mathbf{L}_{\equiv\equiv G}^\dagger, \quad (3)$$

$$\Omega_e = \mathbf{b}_e^\top \mathbf{L}_{\equiv\equiv G}^\dagger \mathbf{b}_e. \quad (4)$$

Hence, if the probabilistic reweight of this edge is chosen such that $\mathbb{E}[f] = 0$, then we have $\mathbb{E}[\mathbf{L}_{\equiv\equiv\tilde{G}}^\dagger] = \mathbf{L}_{\equiv\equiv G}^\dagger$, as desired. Importantly, f remains finite in the following relevant limits:

$$\begin{aligned} \text{deletion:} \quad & \frac{\Delta w}{w_e} \rightarrow -1, & f & \rightarrow (1 - w_e \Omega_e)^{-1} \\ \text{contraction:} \quad & \frac{\Delta w}{w_e} \rightarrow +\infty, & f & \rightarrow -(w_e \Omega_e)^{-1} \end{aligned} \quad (5)$$

3.2 Minimizing the error

Minimizing the magnitude of the change $\Delta \mathbf{L}_{\equiv\equiv}^\dagger$ requires a choice of matrix norm, which we take to be the sum of the squares of the entries (ie, the square of the Frobenius norm). Our motivation is twofold. First, is the algebraically convenient fact that the Frobenius norm of a rank one matrix has a simple form, viz

$$m_e \equiv \|\mathbf{M}_e\|_F = w_e \mathbf{b}_e^\top \mathbf{L}_{\equiv\equiv G}^\dagger \mathbf{L}_{\equiv\equiv G}^\dagger \mathbf{b}_e. \quad (6)$$

⁵This expression is only officially applicable when the initial and final matrices are full-rank; additional care must be taken when they are not. However, as $\mathbf{L}_{\equiv\equiv\tilde{G}}$ and $\mathbf{L}_{\equiv\equiv G}$ share the same kernel, and \mathbf{b}_e is perpendicular to it, the original formula remains valid [19] (so long as the graph remains connected).

Second, the square of this norm behaves as a variance; to the extent that the $\underline{\mathbf{M}}_e$ associated to different edges can be approximated as (entrywise) uncorrelated, one can decompose multiple perturbations as follows:

$$\mathbb{E}\left[\left\|\sum \underline{\Delta\mathbf{L}}^\dagger\right\|_F^2\right] = \sum \mathbb{E}\left[\left\|\underline{\Delta\mathbf{L}}^\dagger\right\|_F^2\right], \quad (7)$$

which greatly simplifies the analysis when multiple reductions are considered (see Section 4).

3.3 Reducing edges and nodes

Depending on the application, one may desire to reduce the number of nodes (ie, coarsen), the number of edges (ie, sparsify), or both.

Let r be the number of relevant items reduced during a particular iteration. When those items are nodes, then $r = r_c = 1$ for a contraction, and $r = r_d = 0$ for a deletion. When those items are edges, then $r = r_d = 1$ for a deletion. However, for a contraction, $r > 1$ is possible; if the contracted edge formed a triangle in the original graph, then the other two edges will become parallel in the reduced graph. With respect to the Laplacian, this is equivalent to a single edge, with weight given by the sum of these parallel edges. Thus, for a contraction, $r = r_c = 1 + \tau_e$, where τ_e is the number of triangles in which the contracted edge e participates.

3.4 A cost function for spectral graph reduction

Motivated by the previous discussions, we seek to minimize the following quantity:

$$\mathcal{C} = \mathbb{E}\left[\left\|\underline{\Delta\mathbf{L}}^\dagger\right\|_F^2\right] - \beta^2 \mathbb{E}[r], \quad (8)$$

subject to

$$\mathbb{E}\left[\underline{\Delta\mathbf{L}}^\dagger\right] = \underline{\mathbf{0}}, \quad (9)$$

where β is a parameter that controls the tradeoff between items reduced and error incurred in the $\underline{\mathbf{L}}^\dagger$.

Let p_d (p_c) be the probability of deleting (contracting) edge e . If the probabilistic change to this edge results in neither deletion nor contraction, it will be reweighted (with probability $1 - p_d - p_c$). Hence, the constraint (9) requires that these reweights satisfy

$$\frac{p_d}{1 - w_e \Omega_e} - \frac{p_c}{w_e \Omega_e} + (1 - p_d - p_c) \mathbb{E}[f | \text{reweight}] = 0, \quad (10)$$

where we have used the limits in (5). Likewise, the cost function (8) for acting on edge e becomes:

$$\mathcal{C} = \left(\frac{p_d}{(1 - w_e \Omega_e)^2} + \frac{p_c}{(w_e \Omega_e)^2} + (1 - p_d - p_c) \mathbb{E}[f^2 | \text{reweight}] \right) m_e^2 - \beta^2 (r_d p_d + r_c p_c). \quad (11)$$

For a fixed p_d and p_c , $\mathbb{E}[f | \text{reweight}]$ is fixed by equation (10), and the inequality $\mathbb{E}[f^2 | \text{reweight}] \geq \mathbb{E}[f | \text{reweight}]^2$ becomes an equality under minimization of (11). Thus, if an edge is to be reweighted, it will be changed by the unique Δw satisfying

$$\frac{p_d}{1 - w_e \Omega_e} - \frac{p_c}{w_e \Omega_e} + (1 - p_d - p_c) \frac{\frac{\Delta w}{w_e}}{1 + \frac{\Delta w}{w_e} w_e \Omega_e} = 0. \quad (12)$$

Clearly, the space of allowed solutions lies within the simplex $\mathcal{S}: 0 \leq p_d, 0 \leq p_c, p_d + p_c \leq 1$. The additional constraint $-1 \leq \frac{\Delta w}{w_e} \leq \infty$ further implies that $p_c \leq w_e \Omega_e$ and $p_d \leq 1 - w_e \Omega_e$. Hence, we substitute (12) into (11), and minimize it over this domain (given the parameters β , m_e , $w_e \Omega_e$, and τ_e).

For a given edge e , there are three regimes for the solution, depending on the value of β (see Table 1 and Table 2). For $\beta < \beta_1(m_e, w_e \Omega_e, \tau_e) = \min(\beta_{1d}, \beta_{1c})$, the edge should not be perturbed. For $\beta > \beta_2(m_e, w_e \Omega_e, \tau_e)$, the optimal probabilistic action leads to either deletion or contraction. In the intermediate case ($\beta_1 < \beta < \beta_2$), if $\beta_{1d} < \beta_{1c}$, the edge is either deleted or reweighted, and if $\beta_{1c} < \beta_{1d}$, the edge is either contracted or reweighted.

$\beta < \beta_1$	$p_d = 0, \quad p_c = 0$
$\beta_1 < \beta < \beta_2$	$p_d = 1 - \frac{m_e}{(1-w_e\Omega_e)\beta}, \quad p_c = 0,$ $\frac{\Delta w}{w_e} = -\frac{p_c}{w_e\Omega_e}$
$\beta_1 < \beta < \beta_2$	$p_d = 0, \quad p_c = 1 - \frac{m_e}{w_e\Omega_e\beta\sqrt{1+\tau_e}},$ $\frac{\Delta w}{w_e} = \left(1 - \frac{p_d}{1-w_e\Omega_e}\right)^{-1} - 1$
$\beta_2 < \beta$	$p_d = 1 - w_e\Omega_e, \quad p_c = w_e\Omega_e$

Table 1: **Actions that minimize \mathcal{C} .** For a given edge e , there are three regimes for the solution, depending on the value of β . For the case when the target items to reduce are the nodes, set $\tau_e = 0$.

	β_{1d}	β_{1c}	β_2
edges	$\frac{m_e}{1-w_e\Omega_e}$	$\frac{m_e}{w_e\Omega_e} \frac{1}{\sqrt{1+\tau_e}}$	$\frac{m_e}{w_e\Omega_e(1-w_e\Omega_e)} \frac{1}{1+\sqrt{1+\tau_e}}$
nodes	\emptyset	$\frac{m_e}{w_e\Omega_e}$	$\frac{m_e}{w_e\Omega_e(1-w_e\Omega_e)}$

Table 2: **Values of β dividing the three regimes.** Note that when the target items to reduce are the edges, the number of triangles enters into the expressions, and when they are the nodes, there is no deletion in the intermediate regime. However, regardless of the target items, both deletion and contraction may have finite probability (eg, if $\beta_2 < \beta$).

3.5 Node weighted Laplacian

Often, when nodes are merged, one represents the connectivity by a matrix of smaller size. To properly compare its spectral properties with those of the original, one must keep track of the number of original nodes that make up these “supernodes” and assign them proportional weights. The appropriate Laplacian is then $\underline{\mathbf{L}} = \underline{\mathbf{W}}_n^{-1} \underline{\mathbf{B}}^\top \underline{\mathbf{W}}_e \underline{\mathbf{B}}$, where the $\underline{\mathbf{W}}$ are the diagonal matrices of node weights⁶ (commonly referred to as the “mass matrix” [21]) and edge weights,

⁶We remark that the use of the random walk matrix $\underline{\mathbf{D}}^{-1} \underline{\mathbf{L}}$ is essentially using node degree as a surrogate for node weights.

respectively, and $\underline{\mathbf{B}}$ is the signed incidence matrix.

Moreover, when updating the $\underline{\mathbf{L}}^\dagger$, one must be careful to choose the appropriate pseudoinverse for this Laplacian, which is given by

$$\underline{\mathbf{L}}^\dagger = (\underline{\mathbf{L}} + \underline{\mathbf{J}})^{-1} - \underline{\mathbf{J}}, \quad (13)$$

$$\underline{\mathbf{J}} = \frac{1}{\underline{\mathbf{1}}^\top \underline{\mathbf{w}}_n} \underline{\mathbf{1}} \underline{\mathbf{w}}_n^\top \quad (14)$$

where $\underline{\mathbf{w}}_n$ is the vector of node weights.

4 Proposed algorithms for graph reduction

Using this framework, we now describe our graph reduction algorithms.

Similar to many graph coarsening algorithms [22, 23], our scheme obtains the reduced graph by acting on the initial graph (as opposed to building it up by adding edges to the empty graph, as in most sparsification algorithms [24, 25]). We first present a simple algorithm that reduces the graph in a single step. We then outline a more general multi-step scheme.

4.1 A single-step algorithm

Algorithm 1 describes the procedure for a single-step reduction. It assumes an appropriate choice of: s , the fraction of edges to be considered for reduction; and β , the parameter controlling the error.

Care must be taken, as multiple deletions or contractions may result in undesirable behavior. For example, while any edge that is itself a cut-set will never be deleted, a collection of edges that together make a cut-set might all have finite deletion probability. Hence, if multiple edges are simultaneously deleted, the graph could become disconnected. Conversely, this algorithm could underestimate the change in the inverse associated with simultaneous contractions. For example, consider two important nodes both connected to the same unimportant node: contracting the unimportant one into either of the other two

Algorithm 1 ReduceGraph

```
1: Inputs: graph  $G$ , sample fraction  $s$ , parameter  $\beta$ 
2: Initialize  $\tilde{G} \leftarrow G$ 
3: Sample  $\lceil s|E| \rceil$  edges uniformly without replacement
4: for (edge  $e$ ) in (sampled edges) do
5:   Compute  $\Omega_e, m_e$  (see equations (4) and (6))
6:   Calculate  $p_d, p_c, \Delta v$  (see Tables 1 and 2)
7:   Probabilistically choose reweight, delete, or contract
8: end for
9: Perform reweights and deletions to  $\tilde{G}$ 
10: Perform contractions to  $\tilde{G}$ 
11: return reduced graph  $\tilde{G}$ 
```

would be fine, but performing both contractions would merge the two important nodes.

We now present a more general multi-step scheme, and a conservative limit that eliminates these issues.

4.2 A multi-step scheme

Algorithm 2 describes our general multi-step scheme. Its inputs are: G , the original graph; s , the fraction of edges to be sampled each iteration; d , the minimum expected decrease in target items per perturbed edge; q , the fraction of sampled edges to be acted upon; and **StopCriterion**, a user-defined function.

With these inputs, we select β implicitly. Let $\beta_{\star,e}$ be the minimum β such that $r_d p_d + r_c p_c \geq d$ for edge e . Each iteration, we compute the $\beta_{\star,e}$ for all sampled edges, and choose a β such that a fraction q of them have $\beta_{\star,e} < \beta$. We then apply the corresponding probabilistic actions to this subset of sampled edges.

We note that s , q , and d could vary as a function of the iteration number, and an appropriate choice could lead to an improved tradeoff between accuracy and running time.

However, we set q such that only the sampled edge with the lowest $\beta_{\star,e}$ is acted upon (ie, $q = 1/\lceil s|E| \rceil$). While likely too conservative, this choice avoids the problems associated with simultaneous reductions. Additionally, we choose to compute \mathbf{L}^\dagger at the onset and update it using the Woodbury matrix identity.

Algorithm 2 ReduceGraphMulti

```
1: Inputs: graph  $G$ , sample fraction  $s$ , minimum  $\mathbb{E}[r]$  per edge perturbed  $d$ , fraction of
   sampled edges to perturb  $q$ , some StopCriterion
2: Initialize  $\tilde{G}_0 \leftarrow G$ ,  $t \leftarrow 0$ ,  $stop \leftarrow \text{False}$ 
3: while not ( $stop$ ) do
4:   Sample  $\lceil s|E| \rceil$  edges uniformly without replacement
5:   for (edge  $e$ ) in (sampled edges) do
6:     Compute  $\Omega_e$ ,  $m_e$  (see equations (4) and (6))
7:     Evaluate  $\beta_{*e}$  (see Tables 1 and 2)
8:   end for
9:   Choose  $\beta$  according to  $q$ 
10:  Probabilistically choose reweight, delete, or contract for each edge  $e$ 
11:  Perform reweights and deletions to  $\tilde{G}_t$ 
12:  Perform contractions to  $\tilde{G}_t$ 
13:   $\tilde{G}_{t+1} \leftarrow \tilde{G}_t$ ,  $t \leftarrow t + 1$ 
14:   $stop \leftarrow \text{StopCriterion}(\tilde{G}_t)$ 
15: end while
16: return reduced graph  $\tilde{G}_t$ 
```

5 Empirical results

In this section, we validate our framework and compare it with existing algorithms. We start by considering two natural limits of our general framework, namely graph sparsification (removing regimes involving edge contraction), and graph coarsening (where the goal is to reduce the number of nodes).

5.1 Comparison with spectral graph sparsification

Figure 1 compares our algorithm (targeting reduction of edges and not considering contraction) with the spectral sparsification algorithm from [11]. We consider the stochastic block model, as there is a clear separation of the eigenvectors associated to the global structure (ie, the communities) and the bulk of the spectrum. Note that these algorithms have different objectives (preserving the $\underline{\mathbf{L}}^\dagger$ and $\underline{\mathbf{L}}$, respectively), and both accomplish their desired goal.

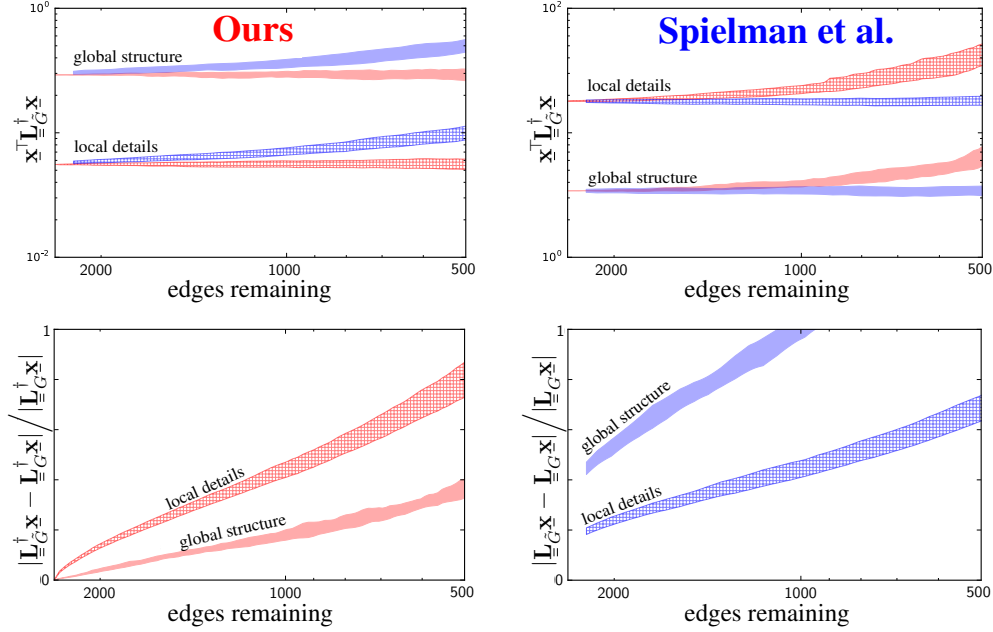


Figure 1: **Validation of our graph reduction algorithm and comparison with spectral sparsification.** We apply our algorithm without contraction (in *red*) and the spectral sparsification algorithm by Spielman et al [11] (in *blue*) to a single instance of the symmetric stochastic block model (256 nodes, 4 communities, and intra- and inter-community connection probabilities 2^{-2} and 2^{-6} , respectively) several times. We combine the 3 nontrivial eigenvectors (“global structure”), centering the shading at their collective mean, ranging $\pm 1\sigma$ of the change from their individual initial values. We combine the remaining eigenvectors in a similar way (“local details”). *Upper left* shows quadratic form using the Laplacian pseudoinverse, and *upper right* the standard quadratic form. Note that the upward bias of the reciprocal metric is expected for both algorithms (as $\mathbb{E}[X] \leq 1/\mathbb{E}[1/X]$ for any random variable $X > 0$). A more discriminating measure is shown in the *bottom* plots, and demonstrates that our algorithm preferentially preserves the global structure (*bottom left*).

5.2 Comparison with spectral graph coarsening

Figure 2 compares our algorithm (targeting reduction of nodes) with a proposed method for spectral graph coarsening [15, 13], which performs k -means clustering on the nodes, using as features the lowest k (nonzero) eigenvectors of the Laplacian. Their reduced Laplacian is given by $\mathbb{C}^\top \mathbb{L}_G \mathbb{C}$, where \mathbb{C} is the mapping from original to coarsened nodes, with entries

$$c_{ij} = \begin{cases} 1 & \text{node } j \text{ in supernode } i \\ 0 & \text{otherwise} \end{cases}$$

We note that while parallel edges are correctly combined by summing their weights, these schemes do not perform any additional reweighting. In general, if one merges nodes without reweighting the edges, the spectrum will increase. However, even when the spectrum is rescaled, its shape is not preserved. Whereas for our algorithm, the reduced graph retains both the magnitude and shape of the lowest Laplacian eigenvalues.

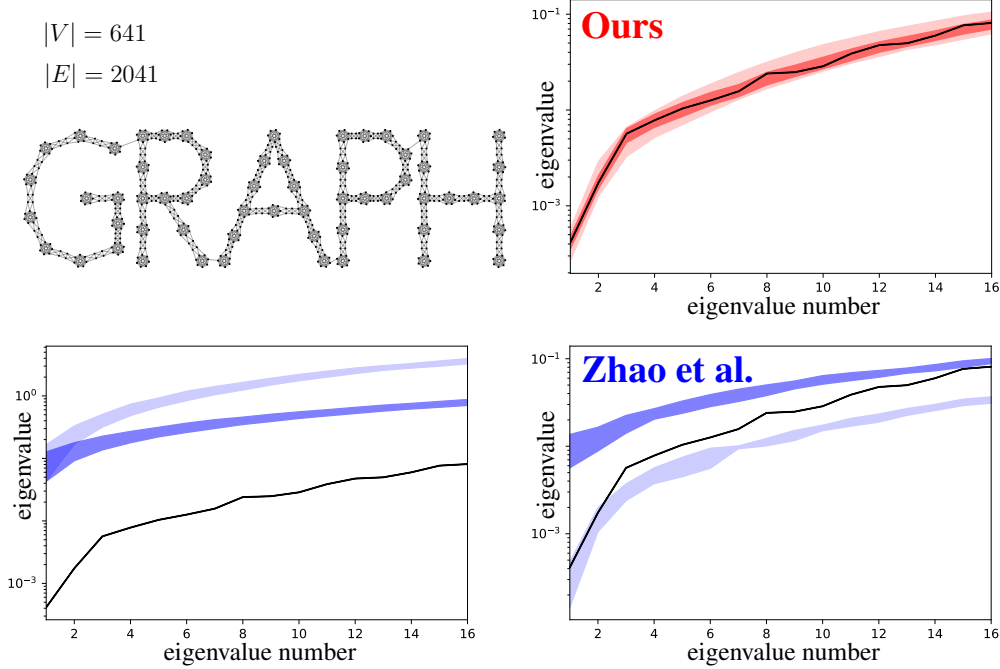


Figure 2: **Comparison with spectral graph coarsening.** We apply our algorithm (targeting reduction of nodes) (*upper right*, in *red*) and the k -means spectral coarsening method by Zhao et al [15] (*bottom*, in *blue*) to the graph in the *upper left*. *Black curve*: 16 lowest eigenvalues of the original graph Laplacian, *heavy shading*: distribution for $3\times$ reduction of nodes, *light shading*: distribution for $12\times$ reduction of nodes. Note that their unnormalized spectrum (*bottom left*) has a consistent upward bias. However, even when the Laplacian is scaled by the node weights (*bottom right*), it does not preserve the shape of the original spectrum.

5.3 Hyperbolic interlude

When comparing a graph G with its reduced approximation \tilde{G} , it is natural to consider how relevant linear operators treat the same input vector. If the vector $\mathbf{L}_{\tilde{G}}\mathbf{x}$ is aligned with $\mathbf{L}_G\mathbf{x}$, the fractional change in the quadratic form is a natural quantity to consider as it corresponds

to the relative change in magnitude of the vector. However, it is not so clear how to compare vectors that have an angular difference. Here, we briefly describe what we believe to be an appropriate extension of this notion of fractional change.

As the action of two Laplacians on the same vector result in a pair of vectors with nonnegative inner product, we draw intuition from the Poincaré half-plane model of hyperbolic geometry. In particular, we orient the plane perpendicular to the first vector and compute the geodesic distance to the second, viz

$$d_h(\underline{\mathbf{x}}, \underline{\mathbf{y}}) = \operatorname{arccosh} \left(1 + \frac{(\underline{\mathbf{x}} - \underline{\mathbf{y}})^\top (\underline{\mathbf{x}} - \underline{\mathbf{y}})}{2 \underline{\mathbf{x}}^\top \underline{\mathbf{y}}} \right). \quad (15)$$

This quantity has several standard desirable features: $d_h(\underline{\mathbf{x}}, \underline{\mathbf{y}}) \geq 0$, $d_h(\underline{\mathbf{x}}, \underline{\mathbf{y}}) = 0 \iff \underline{\mathbf{x}} = \underline{\mathbf{y}}$, and $d_h(\underline{\mathbf{x}}, \underline{\mathbf{y}}) = d_h(\underline{\mathbf{y}}, \underline{\mathbf{x}})$. In addition, if $d_h(\underline{\mathbf{L}}_G \underline{\mathbf{x}}, \underline{\mathbf{L}}_{\tilde{G}} \underline{\mathbf{x}}) \leq \ln(1 + \varepsilon)$ for any eigenvector of $\underline{\mathbf{L}}_G$, then \tilde{G} is an ε -approximation of G . Thus, it captures many aspects of the standard notion of spectral similarity, while additionally considering changes not aligned with $\underline{\mathbf{L}}_G \underline{\mathbf{x}}$.

5.4 Sample fraction s can be small

In Figure 3, we show the effects of varying the sample fraction s on the error incurred in the reduction. This study demonstrates that our metric of edge importance is relevant to the change in $\underline{\mathbf{L}}^\dagger$, as the error decreases with increasing sample size. Conversely, an accurate reduction requires surprisingly few samples per iteration (a trend we noticed in all graphs considered).

5.5 Other datasets

One important application of graph coarsening is data visualization. To this end, we applied our algorithm to several real-world datasets and generated videos of their reduction. Figure 4 displays several stages of our algorithm applied to a temporal social network. Note that our algorithm preserves the overall structure, even when the graph is reduced by a large factor. A video of this reduction can be found [here](#). An application to an airport network, a case with

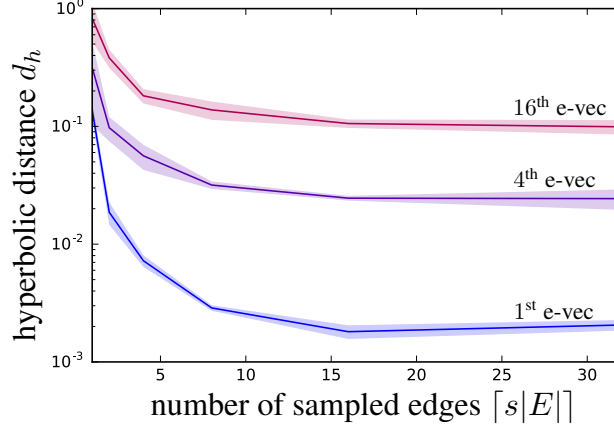


Figure 3: **Effect of sample size on reduction error.** We perform a $2\times$ reduction of nodes on the “GRAPH” graph from Figure 2 for varying number of sampled edges per iteration $\lceil s|E| \rceil$. We measure the hyperbolic distance d_h between $\underline{\mathbf{L}}_{\hat{G}}\mathbf{x}$ and $\underline{\mathbf{L}}_G\mathbf{x}$ for 3 nontrivial eigenvectors \mathbf{x} of the original Laplacian $\underline{\mathbf{L}}_G$ associated to the global structure. Note that a relatively small number of edge samples are required to reduce the error to nearly its asymptotic value.

both geometric and scale-free aspects, can be found [here](#). A condensation of the European road network can be found [here](#), and a graph of the text “GRAPH” can be found [here](#).⁷

6 Conclusion

In this work, we provide a unification of graph sparsification (by edge deletion) and graph coarsening (by edge contraction) using a single objective function: preserving the Laplacian pseudoinverse $\underline{\mathbf{L}}^\dagger$. We provide a framework for graph reduction that uses deletion, contraction, and reweighting to keep $\mathbb{E}[\underline{\mathbf{L}}_{\hat{G}}^\dagger] = \underline{\mathbf{L}}_G^\dagger$, and uses a measure of edge importance to minimize its variance. We demonstrate that our algorithm preferentially preserves the spectral properties associated to the global structure.

⁷Explicit urls for the non-hyperlinked:
[youtube.com/watch?v=qqLJclVUML8](https://www.youtube.com/watch?v=qqLJclVUML8),
[youtube.com/watch?v=tXUr6RBraEI](https://www.youtube.com/watch?v=tXUr6RBraEI),
[youtube.com/watch?v=UVhT0y4Uae0](https://www.youtube.com/watch?v=UVhT0y4Uae0),
[youtube.com/watch?v=i3u4kkxMK40](https://www.youtube.com/watch?v=i3u4kkxMK40)

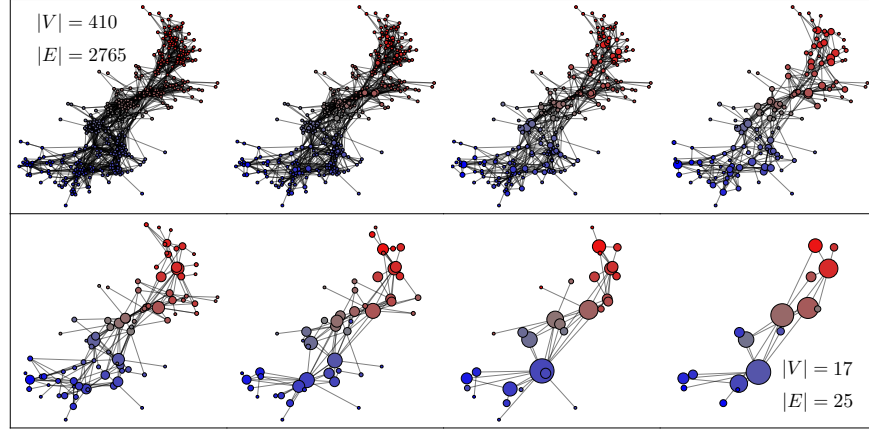


Figure 4: **Our reduction algorithm applied to a social network.** The data are taken from [26], with edge weights proportional to the number of face-to-face interactions during a 12-hour exhibition on infectious diseases. Color indicates lowest nontrivial eigenvector of the Laplacian.

References

- [1] Chazelle, B. *The discrepancy method: randomness and complexity* (Cambridge University Press, 2000).
- [2] Bronstein, M. M., Bruna, J., LeCun, Y., Szlam, A. & Vandergheynst, P. Geometric deep learning: Going beyond euclidean data. *IEEE Signal Processing Magazine* **34**, 18–42 (2017). 1611.08097.
- [3] Bruna, J., Zaremba, W., Szlam, A. & LeCun, Y. Spectral networks and locally connected networks on graphs. In *Proceedings of the International Conference on Learning Representations (ICLR)* (2014).
- [4] Henaff, M., Bruna, J. & LeCun, Y. Deep convolutional networks on graph-structured data. *arXiv:1506.05163* (2015).
- [5] Batson, J., Spielman, D. A., Srivastava, N. & Teng, S.-H. Spectral sparsification of graphs: Theory and algorithms. *Communications of the ACM* **56**, 87–94 (2013).

- [6] Teng, S.-H. The laplacian paradigm: Emerging algorithms for massive graphs. In *Theory and Applications of Models of Computation*, 2–14 (Springer Berlin Heidelberg, 2010).
- [7] Fiedler, M. Algebraic connectivity of graphs. *Czechoslovak Mathematical Journal* **23**, 298–305 (1973).
- [8] Christiano, P., Kelner, J. A., Madry, A., Spielman, D. A. & Teng, S. Electrical flows, laplacian systems, and faster approximation of maximum flow in undirected graphs. In *Proceedings of the 43th Annual ACM Symposium on Theory of Computing (STOC)*, 273–282 (2011).
- [9] Kyng, R., Rao, A., Sachdeva, S. & Spielman, D. A. Algorithms for lipschitz learning on graphs. In *Proceedings of the 28th Annual Computational Learning Theory (COLT)* (2015).
- [10] Spielman, D. A. & Teng, S.-H. Spectral sparsification of graphs. *SIAM Journal on Computing* **40**, 981–1025 (2011).
- [11] Spielman, D. A. & Srivastava, N. Graph sparsification by effective resistances. *SIAM Journal on Computing* **40**, 1913–1926 (2011).
- [12] Loukas, A. & Vandenbroucke, P. Spectrally approximating large graphs with smaller graphs. In *Proceedings of the 35th International Conference on Machine Learning (ICML)*, 3237–3246 (2018).
- [13] Jin, Y. & JaJa, J. F. Network summarization with preserved spectral properties. *arXiv:1802.04447* (2018).
- [14] Purohit, M., Prakash, B. A., Kang, C., Zhang, Y. & Subrahmanian, V. Fast influence-based coarsening for large networks (ACM, 2014).
- [15] Zhao, Z., Wang, Y. & Feng, Z. Nearly-linear time spectral graph reduction for scalable graph partitioning and data visualization. *arXiv:1812.08942* (2018).

- [16] Monnig, N. D. & Meyer, F. G. The resistance perturbation distance: A metric for the analysis of dynamic networks. *Discrete Applied Mathematics* **236**, 347–386 (2018).
- [17] Cohen, M. B. *et al.* Almost-linear-time algorithms for markov chains and new spectral primitives for directed graphs. *arXiv:1611.00755* (2016).
- [18] Oxley, J. G. *Matroid theory*, vol. 3 (Oxford University Press, USA, 2006).
- [19] Riedel, K. S. A sherman–morrison–woodbury identity for rank augmenting matrices with application to centering. *SIAM Journal on Matrix Analysis and Applications* **13**, 659–662 (1992).
- [20] Woodbury, M. A. *Inverting modified matrices*. Memorandum Rept 42, Statistical Research Group (Princeton University, Princeton, NJ, 1950).
- [21] Koren, Y., Carmel, L. & Harel, D. Ace: a fast multiscale eigenvectors computation for drawing huge graphs. In *Proceedings of the IEEE Symposium on Information Visualization*, 137–144 (2002).
- [22] Hendrickson, B. & Leland, R. A multilevel algorithm for partitioning graphs. In *Proceedings of the ACM/IEEE Conference on Supercomputing*, article 28 (1995).
- [23] Ron, D., Safro, I. & Brandt, A. Relaxation-based coarsening and multiscale graph organization. *SIAM Journal on Multiscale Modeling & Simulation* **9**, 407–423 (2011).
- [24] Kyng, R., Pachocki, J., Peng, R. & Sachdeva, S. A framework for analyzing resparsification algorithms. In *Proceedings of the 28th Annual ACM-SIAM Symposium on Discrete Algorithms (SODA)*, 2032–2043 (2017).
- [25] Lee, Y. T. & Sun, H. An sdp-based algorithm for linear-sized spectral sparsification. In *Proceedings of the 49th Annual ACM SIGACT Symposium on Theory of Computing (STOC)*, 678–687 (2017).

- [26] Isella, L. *et al.* What's in a crowd? analysis of face-to-face behavioral networks. *Journal of Theoretical Biology* **271**, 166–180 (2011).